British Journal of Pharmacology

DOI:10.1111/j.1476-5381.2011.01553.x
www.brjpharmacol.org

RESEARCH PAPER

Effects of NMDA receptor antagonists with different subtype selectivities on retinal spreading depression

Minyan Wang[1]*, Paul L Chazot[2]*, Sura Ali[1], Stevens F Duckett[1] and Tihomir P Obrenovitch[3]

[1]*School of Pharmacy and Biomedical Sciences, University of Central Lancashire, Preston, UK,* [2]*School of Biological and Biomedical Science, University of Durham, Durham, UK, and* [3]*School of Pharmacy, University of Bradford, Bradford, UK*

Correspondence
Minyan Wang, Department of Biological Sciences, Xi'an Jiaotong-Liverpool University, 111 Ren Ai Road, Dushu Lake Higher Education Town, Suzhou 215123, China. E-mail: minyan.wang@xjtlu.edu.cn

*Minyan Wang and Paul L Chazot are joint first authors.

Keywords
spreading depression; NMDA receptor subtypes; NVP-AAM077; GluN2A; GluN2A/2B; immunoblotting; chick retina; GluN2B; CP-101,606; GluN2D; UBP141

Received
18 January 2011
Revised
12 May 2011
Accepted
5 June 2011

BACKGROUND AND PURPOSE

Spreading depression (SD) is a local, temporary disruption of cellular ionic homeostasis that propagates slowly across the cerebral cortex and other neural tissues such as the retina. Spreading depolarization associated with SD occurs in different types of stroke, and this phenomenon correlates also with the initiation of classical migraine aura. The aim of this study was to investigate how NMDA receptor antagonists with different subtype selectivity alter SD.

EXPERIMENTAL APPROACH

Immunoblotting was applied to the chick retina for NMDA receptor subunit protein analysis, and an efficient *in vitro* chick retinal model used with SD imaging for NMDA receptor pharmacology.

KEY RESULTS

The prominent NMDA receptor subtypes GluN1, GluN2A and GluN2B were found highly expressed in the chick retina. Nanomolar concentrations of NVP-AAM077 (GluN2A-preferring receptor antagonist) markedly suppressed high K^+-induced SD; that is, ~30 times more effectively than MK801. At sub-micromolar concentrations, Ro 25-6981 (GluN2B-preferring receptor antagonist) produced a moderate SD inhibition, whereas CP-101,606 (also GluN2B-preferring receptor antagonist) and UBP141 (GluN2C/2D-preferring receptor antagonist) had no effect.

CONCLUSIONS AND IMPLICATIONS

The expression of major NMDA receptor subtypes, GluN1, GluN2A and GluN2B in the chick retina makes them pertinent targets for pharmacological inhibition of SD. The high efficacy of NVP-AAM077 on SD inhibition suggests a critical role of GluN2A-containing receptors in SD genesis. Such high anti-SD potency suggests that NVP-AAM077, and other GluN2A-selective drug-like candidates, could be potential anti-migraine agents.

Abbreviations

AOI, area of interest; AUC, area under the curve; CCD, charge-coupled device; CP-101,606, 1-[(1S,2S)-2-hydroxy-2-(4-hydroxyphenyl)-1-methylethyl]-4-phenylpiperidin-4-ol mesylate; CSD, cortical spreading depression; IPP, Image Pro Plus; MK801, (5R,10S)-(+)-5-methyl-10,11-dihydro-5H-dibenzo[a,d]cyclohepten-5,10-imine hydrogen maleate; NVP-AAM077, [(R)-[(S)-1-(4-bromo-phenyl)-ethylamino]-(2,3-dioxo-1,2,3,4-tetrahydro-quinoxalin-5-yl)-methyl]-phosphonic acid; Ro 25-6981, [R-(R*,S*)]-α-(4-hydroxyphenyl)-β-methyl-4-(phenylmethyl)-1-piperidinepropanol hydrochloride hydrate; SD, spreading depression; UBP141, (2R*,3S*)-1-(phenanthrenyl-3-carbonyl)piperazine-2,3-dicarboxylic acid

Introduction

Spreading depression (SD) is a temporary disruption of local ionic homeostasis that propagates slowly across the cerebral cortex, other grey matter regions and the retina. There is now unequivocal electrophysiological evidence that spreading depolarizations associated with SD of electrocorticographic activity occur in different types of stroke (Dreier *et al.*, 2006; Dohmen *et al.*, 2008), and such depolarizing events may favour lesion progression (Risher *et al.*, 2010). There is also convincing clinical data supporting the notion that SD is the pathophysiological correlate of the migraine aura (Olsen, 1995; Ayata, 2010). NMDA receptor antagonists appear as the most effective compounds for SD suppression in experimental models (Gill *et al.*, 1992; Kertész *et al.*, 2010). Clinical data show that ketamine blocks some spreading depolarizations in intensive care stroke patients (Sakowitz *et al.*, 2009), and memantine (another non-competitive NMDA receptor antagonist) is well tolerated when used chronically in Alzheimer's and epilepsy patients (Cammarata and Krusz, 2005; Peltz *et al.*, 2005). However, NMDA receptor antagonists are still perceived as unlikely anti-cortical SD (CSD) candidates for migraine aura treatment because of unacceptable side effects. Given the clinical relevance of SD and the advances in NMDA receptor biology and pharmacology, it is now important and timely to identify, among NMDA receptor antagonists, those that are more likely to be anti-CSD candidates or prototypes.

Subtype selectivity may be a valid approach to improve the ratio, anti-CSD effectiveness versus adverse effects of NMDA receptor antagonists. Indeed, there is pharmacological evidence that the GluN2B subtype plays a role in CSD elicitation and propagation (Menniti *et al.*, 2000; Peeters *et al.*, 2007). The primary aim of the present study was to identify the role of major NMDA receptor GluN2 subtypes in SD elicitation by investigating the effects of several GluN2A, GluN2B and GluN2C/2D-preferring NMDA receptor antagonists on SD in an effective and relevant *in vitro* model, the chick retina preparation.

NMDA receptors are composed of the obligatory GLUN1 subunit in combination with GluN2A–D and GluN3A–B subunits (Monyer *et al.*, 1992). Expression of GluN2 subtypes has been well documented in rodent cortex, which contains primarily GluN2A and GluN2B (Monyer *et al.*, 1992; Dingledine *et al.*, 1999), whereas GluN2C and GluN2D are absent or present at low levels (Dunah *et al.*, 1999; Sun *et al.*, 2000). NMDA receptors are present in the chick retina (Fischer *et al.*, 1998) but little is known of their subtype composition. To test further the validity of the chick retina for this study, an immunological investigation of GluN1, GluN2A, GluN2B and GluN2C/2D subunits was also carried out with chick retina homogenates.

Methods

The drug/molecular target nomenclature conforms to the British Journal of Pharmacology Guide to Receptors and Channels (Alexander *et al.*, 2011).

Validity of the chick retina preparation for CSD NMDA receptor pharmacology

Several elements make the chick retina preparation an effective and relevant *in vitro* model for our study objective: (i) *in vitro* models allow investigators to test several drug concentrations in the same preparation, and the drug concentration at target level is known; (ii) SD waves can be repeatedly initiated by K^+ or NMDA over several hours in the chick retina (Sheardown, 1993; Hanke and de Lima, 2008); (iii) retinal SD can be readily observed and recorded by using its intrinsic optical signal (Dahlem and Müller, 2000; Dahlem *et al.*, 2003; Farkas *et al.*, 2008), and the first phase of the latter signal is quite similar to the corresponding electrophysiological recording (Peixoto *et al.*, 2001; Farkas *et al.*, 2008); and (iv) so far, the NMDA receptor pharmacology of SD in the chick retina (Sheardown, 1993; Kertész *et al.*, 2010) has been found to be very similar, if not identical, to that of CSD (Gill *et al.*, 1992; Kertész *et al.*, 2010).

Chick retina preparation

Male chicks (purchased at 1 day old, Tom Barron Group, Preston, UK) were housed in the animal unit of our institution for at least 1 week before use (aged 8–25 days). All animal care and procedures adhered complied with the Home Office Guidelines and were approved by Ethical Committee of the University of Central Lancashire. As previously described (Farkas *et al.*, 2008), animals were killed by cervical dislocation, the eye dissected at the equator, and the vitreous humour sucked away. The posterior eyecup was placed in a tissue chamber and weighed down to keep it submerged in the perfusion medium. Unless otherwise stated, the chamber was perfused with standard Ringer's solution (mmol·L^{-1} concentrations: 100 NaCl, 6 KCl, 1 $MgSO_4$, 30 $NaHCO_3$, 1 NaH_2PO_3, 1 $CaCl_2$ and 20 glucose; bubbled with 95% O_2 and 5% CO_2; pH 7.3) using a peristaltic pump (Minipuls 3, Anachem, Luton, UK). The perfusion rate was 1 mL·min^{-1} and the medium volume in the chamber kept constant by suction (3a Professional; Kays Medical Limited, Liverpool, UK) through a stainless steel outlet cannula positioned opposite to the perfusion inlet. The tissue was allowed to stabilize in the chamber by perfusion of standard Ringer's solution for at least 30 min before elicitation of the first SD. The temperature was monitored and kept constant at 32°C.

Induction and imaging of spreading depression

Repeated SD (15 in total) were induced at the edge of the eyecup, every 15 min, by 1.2 s ejection of 10 µL of 0.1 mol·L^{-1} KCl through a stainless steel cannula connected to a high-precision syringe pump (CMA/100, CMA/Microdialysis; Solna, Sweden). The retina preparation was illuminated for 5 ms every 1 s using a high-power LED spotlight (625 nm peak wavelength, SLS-0307-A, Mightex; Pleasanton, CA, USA) orientated at 70° angle relative to the perfusion medium surface. The illumination was driven by a computer-controlled power supply (Sirius LED controller, SLC-SA04-U; Mightex, Pleasanton, CA, USA) and the reflected light recorded with a charge-coupled device (CCD) monochrome camera (Qimaging, QICAM model, QIC-F-M-12, 12-bit digital output; Media Cybernetics UK, Marlow,

UK) used at maximal spatial resolution (1 × 1 binning). Image sequences were taken at one frame per second over a 3 min period, started as SD was elicited. The 3 min period allowed us to record the first phase of SD, that is, the transient cellular depolarization associated with propagating SD (Farkas *et al.*, 2008; Hanke and de Lima, 2008). The second, broader and delayed peak of retinal SD intrinsic optical signal (Farkas *et al.*, 2008; Hanke and de Lima, 2008) was overlooked, firstly because the origin and biological significance of this secondary wave remain unclear, and secondly because a much longer recording time (with illumination potentially detrimental to the tissue viability) would have been required. Although the 15 min post-SD delay was unlikely to allow the retina to fully recover from the previous SD, the data show that the preparation was capable of withstanding the repeated SD challenge to which it was subjected well: each local ejection of KCl solution elicited SD successfully, all the SD amplitudes and propagation rates remained within 80% of initial values in control experiments (see Figures 3 and 4, Ringer's values) and those changes were not significant. Camera exposure and illumination were synchronized (5 ms illumination/exposure each second) by using the same external trigger. Camera control together with image acquisition and its storage were carried out using a standard personal computer and Image Pro Plus software (IPP6.3; Media Cybernetics UK, Marlow, UK).

Experimental design for drug testing

Seven series of experiments were carried out to examine the effects of different GluN2 subtype-preferring NMDA receptor antagonists on retinal SD. The well-characterized, non-competitive channel blocker, MK801, was used as reference compound. These series were: (i) Ringer's solution (control, n = 8); (ii) MK801 (n = 7, Sigma-Aldrich, Dorset, UK); (iii) NVP-AAM077 (GluN2A-preferring, n = 7, Novartis Pharma, Basel, Switzerland); (iv) Ro 25-6981 (GluN2B-preferring, n = 8, Sigma-Aldrich, Dorset, UK); (v) CP-101,606 (GluN2B-preferring, n = 6, Axon Medchem BV, Groningen, the Netherlands); (vi) UBP141 (GluN2D-preferring, n = 7, Ascent Scientific, Bristol, UK); and (vii) sodium hydroxide (NaOH series as UBP141 vehicle, n = 6).

To ensure that the selectivity of each drug for its respective preferring NMDA receptor subtype(s) was effective in our study with the chick retina, the concentration range to be tested was carefully selected on the basis of their NMDA receptor subunit selectivity reported in the literature (Table 1). NVP-AAM077 is preferably selective for GluN2A subunit at concentrations less than 0.1 µmol·L^{-1} (Auberson *et al.*, 2002; Liu *et al.*, 2004; Allyson *et al.*, 2010), although lower potencies were reported by other studies (Feng *et al.*, 2004; Paoletti and Neyton, 2007). Accordingly, NVP-AAM077 was tested at the following concentrations: 0.03, 0.1 and 0.3 µmol·L^{-1}. Ro 25-6981 and CP-101,606 are the best-characterized and most widely used antagonists of GluN2B-containing receptors, as they have a >200-fold preference for the latter in comparison to GluN1/2A, GluN1/2C or GluN1/2D receptors (Fischer *et al.*, 1997; Lynch *et al.*, 2001; Chazot *et al.*, 2002). The potency of these compounds in various *in vitro* tissues varies from 0.018 to 10 µmol·L^{-1} (Table 1). Accordingly, the concentrations 1, 3 and 10 µmol·L^{-1} were selected for these two drugs. UBP141

Table 1

Data taken from the literature and our own studies (*in vitro* tests) showing the subtype selectivity of the NMDA receptor antagonists tested in this study, for the different GluN2 subunits

Drugs	GluN2 subunit-preferring	NMDAR subtype selectivity (µmol·L^{-1}) GluN1/GluN2A	GluN1/GluN2B	GluN1/GluN2A/GluN2B	GluN1/GluN2C	GluN1/GluN2D	Preparation where this was studied	Reference
NVP-AAM077	GluN2A	**0.014**	1.8				Recombinant xenopus oocytes	Auberson *et al.*, 2002; Liu *et al.*, 2004
		5.4	67		11.6	37	Recombinant xenopus oocytes	Feng *et al.*, 2004
		0.006	0.06		0.01	0.04	Xenopus oocytes	Neyton and Paoletti, 2006
Ro 25-6981	GluN2A/2B & GluN2B	>30	**0.04**		>30	>30	Rat forebrain membrane	Fischer *et al.*, 1997
		10	**0.018**				Recombinant NMDAR	Lynch *et al.*, 2001
			0.007	**0.0109**			Recombinant HEK cells	Chazot *et al.*, 2002; Hawkins *et al.*, 1999
CP-101,606	GluN2B		**0.039**				Recombinant xenopus oocytes	Mott *et al.*, 1998
		>100	**0.042**		>100	>100	Recombinant HEK cells	Chazot *et al.*, 2002
UBP141	GluN2C/GluN2D					**6.2**	Rat brain synapse	Brothwell *et al.*, 2008
		22	17.2		**5.24**	**2.36**	Rat hippocampal synapse	Costa *et al.*, 2009
MK801	GluN2A = GluNB > GluN2C = GluN2D	0.01	0.01		0.1	0.1	Xenopus oocytes	Yamakura *et al.*, 1993

The use of the bold type is to emphasize the different subtype selectivity of the NMDA receptor antagonists tested in the study for the different GluN2 subunits.

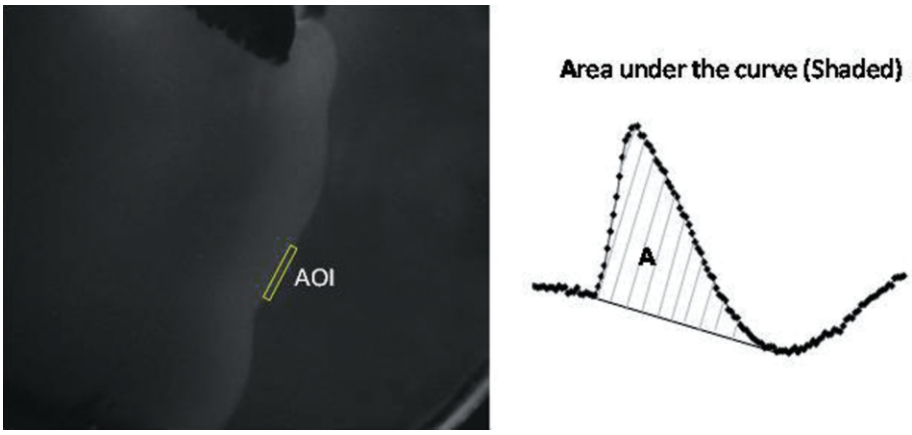

Figure 1

Representative image (left) and plot of SD wave (right; i.e. kinetic of change in grey level intensity within the selected area) induced by high K^+ in the chick retina preparation. The same area of interest (rectangle within left picture, AOI) was selected and used for all pictures of the sequence under study. All the averaged grey levels within the AOI were plotted against time to generate the SD wave plot (right). From these plots, the area under the curve (right panel) of SD wave front were determined by image analysis and used to quantify the drug effects.

shows ninefold selectivity for GluN2D- over GluN2A-containing receptors and sevenfold over GluN2B-containing receptors, but it does not discriminate between GluN2C and GluN2D (Table 1). On the basis of the data displayed in Table 1, the concentrations 1, 3 and 10 $\mu mol \cdot L^{-1}$ were also selected for UBP141 to ensure effectiveness and favour selectivity for NR2C- and NR2D-containing receptors. Accordingly, in the UBP141 vehicle group, 2, 6, 20 $\mu mol \cdot L^{-1}$ of NaOH were applied in respective order. To summarize, all the drugs were tested at three different concentrations (1, 3 and 10 $\mu mol \cdot L^{-1}$), except NVP-AAM077 which was used at ~30 times lower concentrations (0.03, 0.1 and 0.3 $\mu mol \cdot L^{-1}$).

Fifteen SD in total were elicited in each experiment, with three separate SD elicited for each of the different and consecutive tests: (i) initial Ringer's control; (ii) low concentration of drug or vehicle; (iii) medium concentration of drug or vehicle; (iv) high concentration of drug or vehicle; and (v) post-treatment with Ringer's control (i.e. drug removal). A recovery of 15 min followed each SD elicitation. For each test sequence (i.e. elicitation of three SD), whenever required, the perfusion medium was changed immediately after the end of the third SD recording, thus ensuring that the preparation was adequately perfused with the proper drug or Ringer's medium for the subsequent test.

Data analysis and statistical procedures

For each 180-frame sequence, an area of interest (AOI) parallel to the SD wave front was delineated manually; this part of the recorded signal is synchronous of the sudden cellular depolarization that characterizes SD (Farkas *et al.*, 2008). For each picture within the sequence, the grey levels of the pixels constituting the AOI were averaged and corrected by subtracting those of dark background (Dahlem and Müller, 2000). The changes in this value were then plotted against time (i.e. 180 data points over 3 min), providing the kinetics of changes in intrinsic optical signal within the AOI (Figure 1, right).

For each SD wave, the area under the curve (AUC, Grey levels × min, Figure 1, left) was calculated and used as an index of its magnitude. In each image sequence related to a given SD, the distance between the front of the same SD wave measured in two images (captured within 30 to 40 s of each other), divided by the difference in their exposure time, allowed the calculation of SD propagation rate. The calculated values within each different test were averaged and all corresponding data were given as mean ± s.d. in percentage of their respective baselines, that is, averaged value for the first three K^+ stimuli. Kruskal–Wallis test was used for comparison of AUC and propagation rate of SD between the drug and respective vehicle group. Paired *t*-test was used to test the significance of the difference for the last two tests with each drug (i.e. effect of drug removal).

Immunoblotting

Following rapid dissection, chick retina were immediately frozen in liquid nitrogen and then stored at –80°C. Samples were prepared by applying the chloroform/methanol extraction procedure of protein precipitation to chick retina homogenates. Generation and characterization of anti-GluN1, anti-GluN2A, anti-GluN2B and anti-GluN2C/GluN2D antibodies were as previously described (Thompson *et al.*, 2002). All antibodies were used at a final protein concentration of 0.5–1 $\mu g \cdot mL^{-1}$. Rabbit immunoglobulin horseradish peroxidase-linked whole antibody (Amersham Life Sciences, UK) was used at a final dilution of 1:2000. Enhanced chemiluminescence and Western blotting detection system (Amersham Life Sciences, UK) were used to analyse samples in the presence and absence of the peptide to which the antibodies were raised. Samples of whole mouse brain were also analysed and used as positive controls (Thompson *et al.*, 2002). All the animal procedures

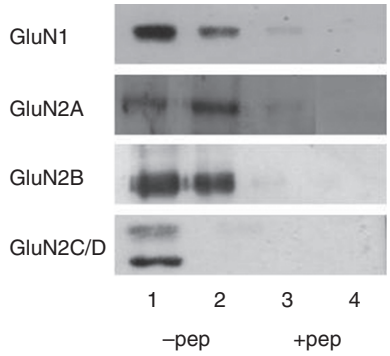

Figure 2

Immunoblot detection of major NMDA receptor subunits in the chick retina. Adult mouse whole brain (lanes 1 and 3, positive control) and chick retina (lanes 2 and 4) homogenates were analysed by immunoblotting. Anti-GluN1, GluN2A, GluN2B and anti-GluN2C/D were used as probes (1 $\mu g \cdot mL^{-1}$ antibody concentration) either in the absence of (–pep), or pre-absorbed with, respective NMDA receptor subunit immune peptides (+pep).

related to this part of the study were in strict accordance with the ethical policies of University of Durham and the Home Office guidelines.

Results

NMDA receptor subtypes in the chick retina

To confirm the validity of our immunoblotting method, adult mouse whole brain samples were analysed for the NMDA receptor subunits GluN1 and GluN2A–D. In the absence of respective NMDA receptor subunit immune peptides, all these major NMDA receptor subtypes were detected in the brain samples (Figure 2, lane 1), which agrees with previous studies (Thompson *et al.*, 2002). In contrast, in the chick retina, GluN1, GluN2A and GluN2B, but not GluN2C/2D, were expressed (Figure 2, lane 2). As expected, following pre-absorption with respective NMDA receptor subunit immune peptides, the NMDA receptor subtypes under study were no longer or barely detectable in either mouse brain or chick retina samples (Figure 2, lanes 3 and 4).

Further validation of SD imaging in the retina preparation for NMDA receptor SD pharmacology

Within each experiment of the control group (Ringer's solution, $n = 8$), all SD induced by high K^+ were associated with a transient increase in the intensity of reflected light (Figure 1, left), a marked change that was clearly visible with the naked eye. The kinetics of changes for the 15 repeated SD was very reproducible within each control experiment. In this group, the AUC (Figure 1, left) and propagation rate for the first three SD waves elicited was 3559 ± 1003 Gl·min (Grey levels × min) and 3.8 ± 1.0 $mm \cdot min^{-1}$ respectively. There was no significant difference in any of these parameters over the five different tests (Figures 3 and 4). This suggests that the 15 min period separating each SD elicitation allowed an appropriate recovery of the retina from previous SD, and that the preparation tolerated well up to 15 consecutive SD in our experimental conditions. We acknowledge the quite large variability of both SD magnitude and velocity data. As the variability was more pronounced between experiments rather than within individual experiment, it could be linked to the quality of the eye dissection and handling of the retina preparation before the experimental procedure.

To verify that our experimental setup was suitable for NMDA receptor pharmacological tests, we examined the effects of MK801, a well-characterized, potent and selective NMDA receptor antagonist previously shown to suppress both cortical and retinal SD (Marrannes *et al.*, 1988; Gill *et al.*, 1992; Willette *et al.*, 1994; Kertész *et al.*, 2010). MK801 significantly reduced the magnitude of retinal SD in a concentration-dependent manner (Figure 3A, $n = 7$). At 10 $\mu mol \cdot L^{-1}$, the drug reduced the magnitude to 24.3% of initial levels (i.e. first three K^+ stimuli with drug-free medium). This effect persisted after drug removal (i.e. last three K^+ stimuli), with SD magnitude remaining at 22.8% of initial levels. The propagation rate of SD was also slightly slower under MK801 application, although this effect did not reach significance (Figure 4) possibly because of the large variability of the data within groups.

Suppression of SD by NVP-AAM077

The GluN2A-preferring NMDA receptor antagonist, NVP-AAM077, was found to be a remarkably potent inhibitor of retinal SD. Indeed, nanomolar concentrations of this drug markedly reduced both the magnitude and propagation rate of SD (Figures 3A and 4, $n = 7$). The suppression of SD by NVP-AAM077 was concentration-dependent. At the maximum concentration tested (0.3 $\mu mol \cdot L^{-1}$), the magnitude and propagation rate were reduced to 31.5% and 52.5% of initial values respectively. SD elicitation and propagation recovered significantly after the removal of NVP-AAM077 (fifth test): the magnitude and propagation rate of SD returned to 79.0% and 91.5% of initial values respectively (Figures 3A and 4; paired *t*-test, $P < 0.05$, comparison of the fifth test vs. the fourth test).

Suppression of SD by Ro 25-6981 but not CP-101,606

At the highest concentration tested (10 $\mu mol \cdot L^{-1}$), Ro 25-6981 reduced significantly the magnitude of retinal SD, to 51.1% of initial values (Figure 3B, $P < 0.05$ respectively, $n = 9$). This inhibitory effect persisted after removal of Ro 25-6981 (fifth test), with the magnitude of SD remained at 58.5% of initial values. The propagation rate of SD had a tendency to be slower with 10 $\mu mol \cdot L^{-1}$ Ro 25-6981, but this reduction (75.1% of initial values) did not reach significance (Figure 4B).

In contrast to Ro 25-6981, CP-101,606 at all concentrations tested did not alter either the magnitude (Figure 3B) or the propagation rate of retinal SD (Figure 4B).

Lack of inhibitory effect of UBP141 on retinal SD

In the UBP141-vehicle group ($n = 6$), NaOH at the concentrations of 2, 6 and 20 $\mu mol \cdot L^{-1}$ did not alter the magnitude of

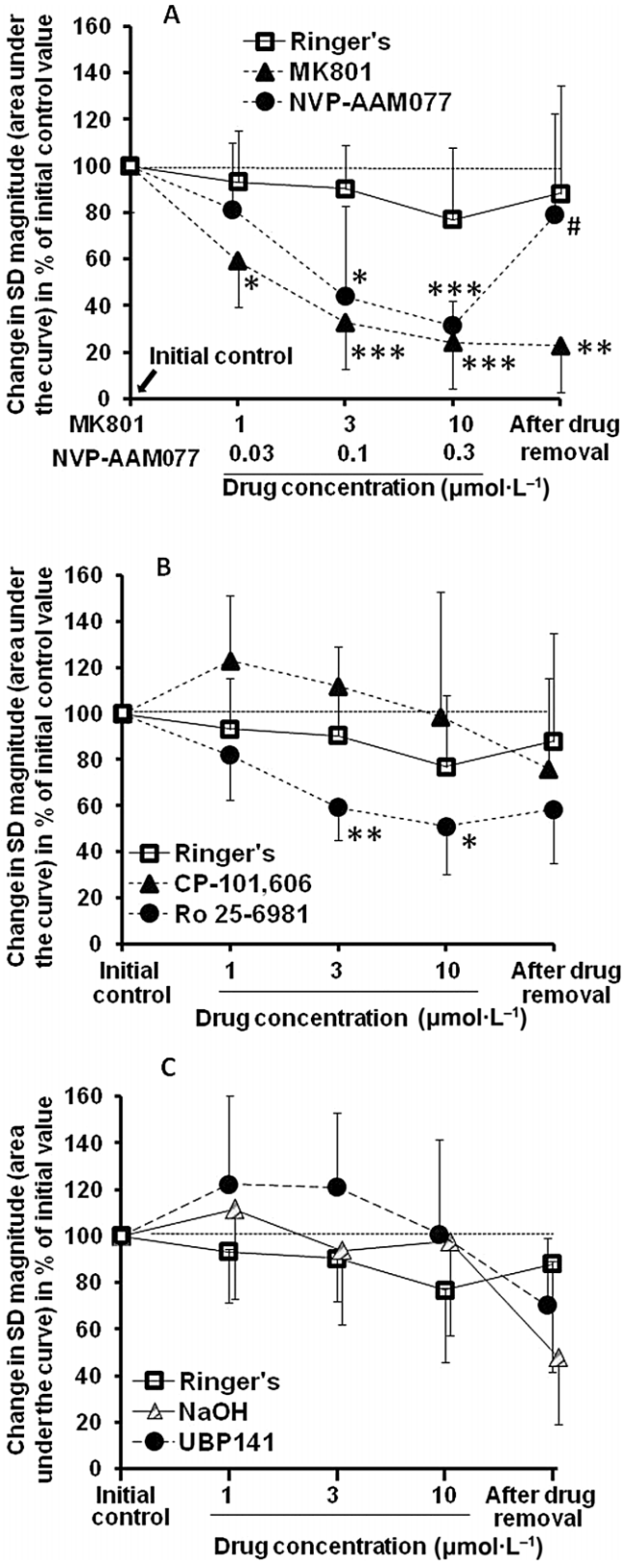

Figure 3

Comparison of the effects of several NMDA receptor antagonists, with different GluN2 subtype selectivity, on the magnitude (area under the curve) of SD induced by K^+ in the chick retina. Seven groups were considered, including two control groups (Ringer's solution, $n = 8$; NaOH as UBP141 sodium hydroxide solution vehicle group, $n = 6$) and five drug treatment groups: MK-801 ($n = 7$), NVP-AAM077 ($n = 7$), CP-101,606 ($n = 6$), Ro 25-6981 ($n = 8$) and UBP141 ($n = 7$). Fifteen SD in total were elicited and five successive perfusion media tested in each experiment: initial Ringer's solution, three different drug concentrations and Ringer's solution (i.e. after drug removal). All the drugs were tested at 1, 3 and 10 µmol·L^{-1}, except NVP-AAM077 whose higher potency required much lower concentrations (0.03, 0.1 and 0.3 µmol·L^{-1}). Data (mean ± SD) are plotted as percentage of their initial levels (averaged value for the first three K^+ stimuli). *$P < 0.05$, **$P \leq 0.01$, ***$P \leq 0.001$ (Kruskal–Wallis test) comparison with control group, except for UBP141 which was compared to its own vehicle (NaOH group). #$P < 0.05$, paired *t*-test used to test whether the susceptibility of the preparation to SD elicitation was significantly restored after the removal of NVP-AAM077.

SD. However, a slight but significant increase in the propagation rate of SD (126% relative to initial levels, $P < 0.05$) was observed at 20 µmol·L^{-1} (i.e. highest NaOH concentration tested, Figure 4C). Re-perfusion with Ringer's solution for the last three K^+ stimuli in this group (i.e. removal of NaOH at fifth test) led to a slight, but non-significant reduction of SD magnitude to 48% of initial levels (Figure 3C). UBP141 at all concentrations tested did not alter either the magnitude (Figure 3C) or propagation rate (Figure 4C) of SD wave in the chicken retina preparation.

Discussion and conclusions

NMDA receptor subtype expression in chick retina – comparison to the cerebral cortex

Our results demonstrate an abundant expression of GluN1, GluN2A and GluN2B subunit in the chick retina; in contrast, GluN2C/GluN2D proteins were not detectable. These data complement previous studies carried out with the retina of chicks (Fischer *et al.*, 1998), rats (Fletcher *et al.*, 2000) and frogs (Vitanova, 2011). The distinct GluN2 subunit composition of the chick retina is similar to that of the rodent cerebral cortex, as the latter is also rich in GluN2A and GluN2B (Monyer *et al.*, 1992; Dingledine *et al.*, 1999) and with low or undetectable GluN2C and GluN2D levels (Dunah *et al.*, 1999; Sun *et al.*, 2000). All together, these data support the notion that the NMDA receptor subtype composition is quite similar in retina and cortex. This is an important feature if one wants to extrapolate pharmacological data obtained in the retina to the cortex. As the GluN1 subunit is an ubiquitous and necessary component of all NMDA receptors, we can already propose that the GluN2A and GluN2B subtypes may be pertinent NMDA receptor targets for suppression or modulation of SD.

The GluN2A subunit is critical to SD elicitation and propagation

NVP-AAM077 (GluN2A-selective) was ~30-fold more potent than MK801 as 'anti-SD' in the chick retina, and the rapid reversibility of NVP-AAM077 effects suggested a competitive

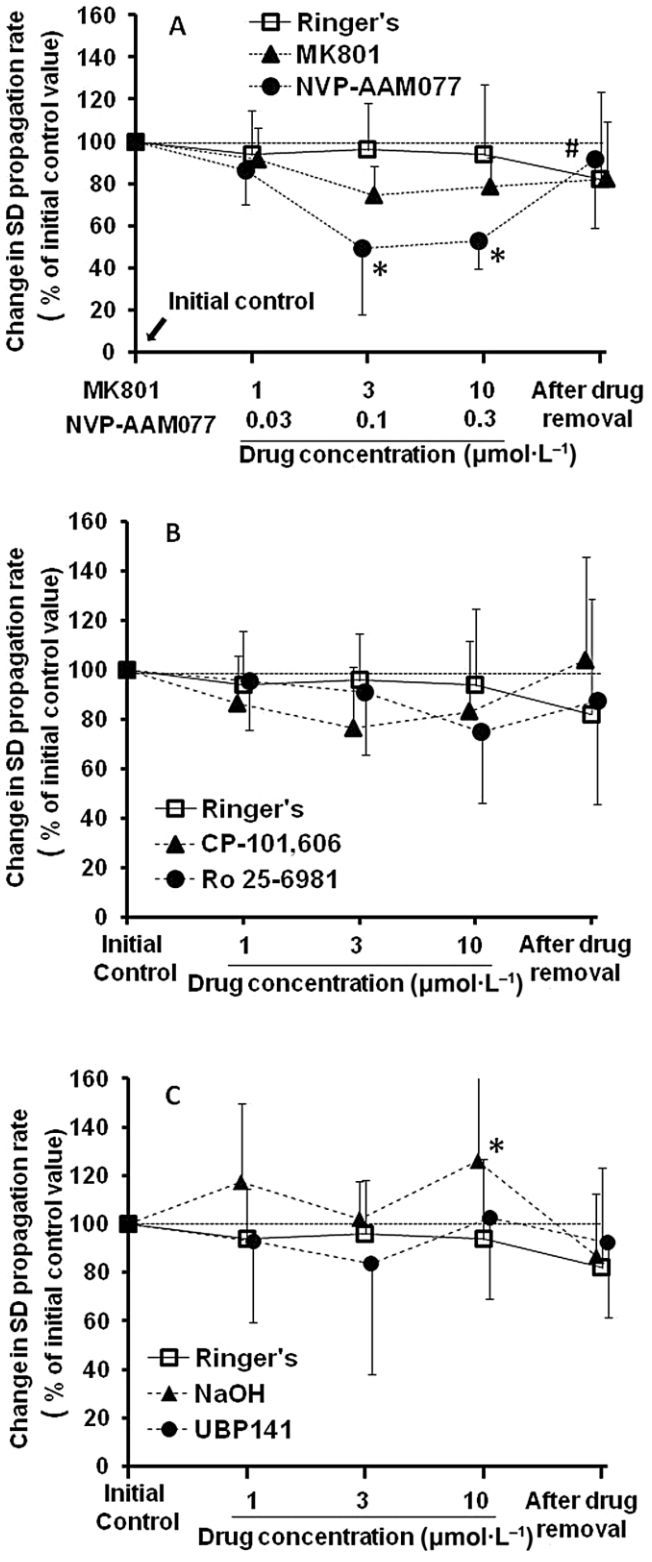

Figure 4

Comparison of the effects of the GluN2A-preferring NMDA receptor antagonist, NVP-AAM077 with that of MK801, on the propagation rate of SD induced by high K^+ in the chick retina. Seven groups and five drug groups were applied as described in Figure 3. Fifteen SD in total were elicited with five successive perfusion media tested in each experiment: initial Ringer's solution, three different drug concentrations and Ringer's solution (i.e. after drug removal). All the drugs were tested at 1, 3 and 10 µmol·L^{-1}, except NVP-AAM077 with higher potency, requiring lower concentrations (0.03, 0.1 and 0.3 µmol·L^{-1}). Data are plotted in means ± SD (as percentage) of averaged values relative to their respective baselines. *$P < 0.05$ (Kruskal–Wallis test) comparison with control group, except for UBP141 which was compared to its own vehicle (NaOH group, $n = 6$). #$P < 0.05$, paired t-test was used to test whether the sensitivity of the preparation to SD elicitation was significantly restored after the removal of NVP-AAM077.

antagonism. The latter feature agrees with the previous demonstration that NVP-AAM077 interacts with the agonist (glutamate/NMDA) domain of GluN2A subunits (Liu *et al.*, 2004; Frizelle *et al.*, 2006). The high efficacy of SD inhibition by NVP-AAM077 suggests a critical role of GluN2A-containing receptors in SD elicitation and propagation. The role of GluN2A in SD genesis was suggested previously by the report that memantine, a non-competitive GluN2A subunit antagonist (Chen and Lipton, 2005), suppressed high K^+-induced CSD in rats (Peeters *et al.*, 2007); preliminary experiments also showed some efficacy of this drug against migraine (Cammarata and Krusz, 2005). Used at 0.3 µmol·L^{-1} in our study, NVP-AAM077 was approximately 320-fold more potent than memantine tested *in vivo* for SD inhibition (brain concentration of ~96 µmol·L^{-1}, Peeters *et al.*, 2007). Such a high anti-SD potency suggests that NVP-AAM077 and drug-alike candidates could be useful as a prophylactic in migraine treatment. In addition, GluN2A subtype selectivity and rapid drug-effect reversibility may contribute to a better safety profile, relative to non-subtype-selective NMDA receptor antagonists. Further *in vivo* investigations are required to examine this possibility. In this case, emphasis would need to be placed on susceptibility to SD initiation (e.g. threshold for SD initiation, latency of SD elicitation after stimulus; van den Maagdenberg *et al.*, 2004) rather than on variables related to progressing SD waves.

GluN2B-containing receptors and SD

Ro 25-6981, which binds to GluN2B-containing receptors (Fischer *et al.*, 1997; Lynch *et al.*, 2001), suppressed retinal SD (Figure 3B). These data suggest that GluN2B subunit also plays a key role in SD genesis. This notion agrees with previous reports showing that Ro 25-6981 inhibited K^+-induced CSD in rats (Peeters *et al.*, 2007). It is of relevance to note that neither blockade of GluN2A (NVP-AAM077) nor GluN2B (Ro 25-6981) led to a complete inhibition of SD in the chick retina. At the highest concentration tested, residual SD magnitude was 31.5% and 51.1% of control with NVP-AAM077 and Ro 25-6981, respectively (Figure 3A and B). The finding that complete suppression of retinal SD was not achieved with any of the NMDA receptor antagonists tested is compatible with the notion that some of the transmembrane ion fluxes associated with SD may not be NMDA receptor-mediated, as discussed previously by Peeters *et al.* (2007). According to Petzold *et al.* (2005), relatively small increases in baseline potassium (~3–7 mmol·L^{-1} *in vivo*) rendered SD resistant to NMDA receptor antagonists. Such interference, linked to the KCl used for SD elicitation, was unlikely in our experi-

ments: firstly, because the small volume ejected was rapidly diluted by the perfusion medium and, secondly, because the recording site was relatively remote from the elicitation site. The very high potency of NVP-AAM077, and the fact that it suppressed retinal SD to a lower residual level than Ro 25-6981 (high efficacy), indicate a dominant role of GluN2A relative to GluN2B in SD elicitation and propagation. It would be pertinent to examine whether the co-application of GluN2A- and GluN2B-selective receptor antagonists results in any synergistic inhibition of SD (e.g. complete suppression of SD).

Conflicting effects of CP-101,606 on SD in the chick retina and in vivo *rat cortex*

In contrast to Ro 25-6981, CP-101,606 did not alter retinal SD (Figure 3B). This set of results is in apparent contradiction with the inhibitory effect of both drugs on CSD induced *in vivo* by electrical stimulation (Menniti *et al.*, 2000) or high K^+ (Peeters *et al.*, 2007). One possible explanation may be linked to the different selectivity of these drugs for different GluN2B-containing heteromers: (i) Ro 25-6981 suppresses NMDA receptor function associated with any GluN2B-containing heteromer (GluN1/GluN2A/GluN2B or GluN1/GluN2B); and (ii) CP-101,606 is potentially more selective, as it appears to only interact with the GluN1/GluN2B diheteromeric form(s) (Chazot *et al.*, 2002). However, this would also imply that GluN1/GluN2B diheteromeric receptors are lacking (or only present at very low levels) in the chicken retina. Rodent cortex data showed that GluN2B proteins exist in both GluN1/GluN2A/2B triheteromeric and GluN1/2B diheteromeric forms of receptors (Chazot *et al.*, 2002), but how the GluN2B proteins are combined in retinal NMDA receptors remains unknown.

Taken together, our data support the notion that normal function of the triheteromeric GluN1/GluN2A/GluN2B form(s) is required for the genesis of retinal SD. They also suggest that the chick retina preparation, although useful, may not be considered as a 'perfect' model for CSD NMDA receptor pharmacology.

GluN2C/GluN2D subtypes and retinal SD

UBP141, which preferably antagonizes GluN2C/GluN2D subunits (Costa *et al.*, 2009), did not alter retinal SD elicitation and propagation. This lack of effect probably resulted from the absence of GluN2C/GluN2D proteins in the chick retina (Figure 2, lane 2). At low micromolar concentrations, UBP141 was also reported to block GluN2B diheteromeric receptors (Morley *et al.*, 2005), but this would be irrelevant if one accepts that GluN1/GluN2B is not present in the chick retina, as proposed above.

Conclusions

As in the cerebral cortex, high levels of GluN1, GluN2A and GluN2B are expressed in the chick retina, making them pertinent targets for pharmacological inhibition of SD. The impressive inhibition of SD by the GluN2A-selective NMDA receptor antagonist, NVP-AAM077, suggests a critical role for GluN2A-containing receptors in SD genesis. Further studies are necessary to establish whether NVP-AAM077 and other drugs of this type are as effective anti-SD compounds *in vivo*, and whether such action is devoid of associated adverse behavioural effects.

Acknowledgements

We greatly thank Dr Yves Auberson from Novartis Pharmas (Basel, Switzerland) for his generous gift, NVP-AAM077 and Rachel Stevens (School of Pharmacy, University of Central Lancashire) for her technical assistance. SA and SFD were supported by central research fund from University of Central Lancashire, Preston, UK. This work was partly funded by BBSRC (UK).

Conflicts of interest

The authors state no conflict of interest.

References

Alexander SPH, Mathie A, Peters JA (2011). Guide to Receptors and Channels (GRAC), 5th edition. Br J Pharmacol 164: S1–S324.

Allyson J, Dontigny E, Auberson Y, Cyr M, Massicotte G (2010). Blockade of NR2A-containing NMDA receptors induces Tau Phosphorylation in rat hippocampal slices. Neural Plast 2010: 340168.

Auberson YP, Allgeier H, Bischoff S, Lingenhoehl K, Moretti R, Schmutz M (2002). 5-Phosphonomethylquinoxalinediones as competitive NMDA receptor antagonists with a preference for the human 1A/2A, rather than 1A/2B receptor composition. Bioorg Med Chem Lett 12: 1099–1102.

Ayata C (2010). Cortical spreading depression triggers migraine attack: pro. Headache 50: 725–730.

Brothwell SL, Barber JL, Monaghan DT, Jane DE, Gibb AJ, Jones S (2008). NR2B- and NR2D-containing synaptic NMDA receptors in developing rat substantia nigra pars compacta dopaminergic neurones. J Physiol 6: 739–750.

Cammarata D, Krusz JC (2005). Memantine: novel mechanism for migraine and headache prophylaxis. Headache 45: 820.

Chazot PL, Lawrence S, Thompson CL (2002). Studies on the subtype selectivity of CP-101,606: evidence for two classes of NR2B-selective NMDA receptor antagonists. Neuropharmacology 42: 319–324.

Chen HS, Lipton SA (2005). Pharmacological implications of two distinct mechanisms of interaction of memantine with N-methyl-D-aspartate-gated channels. J Pharmacol Exp Ther 314: 961–971.

Costa BM, Feng B, Tsintsadze TS, Morley RM, Irvine MW, Tsintsadze V *et al.* (2009). N-methyl-D-aspartate (NMDA) receptor NR2 subunit selectivity of a series of novel piperazine-2,3-dicarboxylate derivatives: preferential blockade of extrasynaptic NMDA receptors in the rat hippocampal CA3-CA1 synapse. J Pharmacol Exp Ther 331: 618–626.

Dahlem MA, Müller SC (2000). Image processing techniques applied to excitation waves in the chicken retina. Methods 21: 317–323.

Dahlem YA, Dahlem MA, Mair T, Braun K, Müller SC (2003). Extracellular potassium alters frequency and profile of retinal spreading depression waves. Exp Brain Res 152: 221–228.

Dingledine R, Borges K, Bowie D, Traynelis SF (1999). The glutamate receptor ion channels. Pharmacol Rev 51: 7–61.

Dohmen C, Sakowitz OW, Fabricius M, Bosche B, Reithmeier T, Ernestus RI *et al.* (2008). Spreading depolarisations occur in human ischemic stroke with high incidence. Ann Neurol 63: 720–728.

Dreier JP, Woitzik J, Fabricius M, Bhatia R, Major S, Drenckhahn C *et al.* (2006). Delayed ischaemic neurological deficits after subarachnoid haemorrhage are associated with clusters of spreading depolarisations. Brain 129 (Pt 12): 3224–3237.

Dunah AW, Yasuda RP, Luo J, Wang Y, Prybylowski KL, Wolfe BB (1999). Biochemical studies of the structure and function of the N-methyl-D-aspartate subtype of glutamate receptors. Mol Neurobiol 19: 151–179.

Farkas E, Pratt R, Sengpiel F, Obrenovitch TP (2008). Direct, live imaging of cortical spreading depression and anoxic depolarisation using a fluorescent, voltage-sensitive dye. J Cereb Blood Flow Metab 28: 251–262.

Feng B, Tse HW, Skifter DA, Morley R, Jane DE, Monaghan DT (2004). Structure-activity analysis of a novel NR2C/NR2D-preferring NMDA receptor antagonist: 1- (phenanthrene-2-carbonyl) piperazine-2,3-dicarboxylic acid. Br J Pharmacol 141: 508–516.

Fischer G, Mutel V, Trube G, Malherbe P, Kew JN, Mohacsi E *et al.* (1997). Ro 25-6981, a highly potent and selective blocker of N-methyl-D-aspartate receptors containing the NR2B subunit. Characterization *in vitro*. J Pharmacol Exp Ther 283: 1285–1292.

Fischer AJ, Seltner RL, Poon J, Stell WK (1998). Immunocytochemical characterization of quisqualic acid- and N-methyl-D-aspartate-induced excitotoxicity in the retina of chicks. J Comp Neurol 393: 1–15.

Fletcher EL, Hack I, Brandstätter JH, Wässle H (2000). Synaptic localization of NMDA receptor subunits in the rat retina. J Comp Neurol 420: 98–112.

Frizelle PA, Chen PE, Wyllie DJ (2006). Equilibrium constants for (R)-[(S)-1-(4-bromo- phenyl)-ethylamino](2,3-dioxo-1,2,3,4-tetrahydroquinoxalin-5-yl)-methyl]-phosphonic acid (NVP-AAM077) acting at recombinant GLUN1/NR2A and GLUN1/NR2B N-methyl-D-aspartate receptors: implications for studies of synaptic transmission. Mol Pharmacol 70: 1022–1032.

Gill R, Andiné P, Hillered L, Persson L, Hagberg H (1992). The effect of MK-801 on cortical spreading depression in the penumbral zone following focal ischaemia in the rat. J Cereb Blood Flow Metab 12: 371–379.

Hanke W, de Lima VM (2008). Central nervous tissue: an excitable medium. A study using the retinal spreading depression as a tool. Philos Transact A Math Phys Eng Sci 366: 359–368.

Hawkins LM, Chazot PL, Stephenson FA (1999). Biochemical evidence for the co-association of three N-methyl-D-aspartate (NMDA) R2 subunits in recombinant NMDA receptors. J Biol Chem 274: 27211–27218.

Kertész S, Kapus G, Gacsályi I, Lévay G (2010). Deramciclane improves object recognition in rats: potential role of NMDA receptors. Pharmacol Biochem Behav 94: 570–574.

Liu L, Wong TP, Pozza MF, Lingenhoehl K, Wang Y, Sheng M *et al.* (2004). Role of NMDA receptor subtypes in governing the direction of hippocampal synaptic plasticity. Science 304: 1021–1024.

Lynch DR, Shim SS, Seifert KM, Kurapathi S, Mutel V, Gallagher MJ *et al.* (2001). Pharmacological characterization of interactions of RO 25-6981 with the NR2B (epsilon2) subunit. Eur J Pharmacol 416: 185–195.

Marrannes R, Willems R, De Prins E, Wauquier A (1988). Evidence for a role of the N-methyl-D-aspartate (NMDA) receptor in cortical spreading depression in the rat. Brain Res 457: 226–240.

Menniti FS, Pagnozzi MJ, Butler P, Chenard BL, Jaw-Tsai SS, Frost White W (2000). CP-101,606, an NR2B subunit selective NMDA receptor antagonist, inhibits NMDA and injury induced c-fos expression and cortical spreading depression in rodents. Neuropharmacology 39: 1147–1155.

Monyer H, Sprengel R, Schoepfer R, Herb A, Higuchi M, Lomeli H *et al.* (1992). Heteromeric NMDA receptors: molecular and functional distinction of subtypes. Science 256: 1217–1221.

Morley RM, Tse HW, Feng B, Miller JC, Monaghan DT, Jane DE (2005). Synthesis and pharmacology of N1-substituted piperazine-2,3-dicarboxylic acid derivatives acting as NMDA receptor antagonists. J Med Chem 48: 2627–2637.

Mott DD, Doherty JJ, Zhang S, Washburn MS, Fendley MJ, Lyuboslavsky P *et al.* (1998). Phenylethanolamines inhibit NMDA receptors by enhancing proton inhibition. Nat Neurosci 1: 659–667.

Neyton J, Paoletti P (2006). Relating NMDA receptor function to receptor subunit composition: limitations of the pharmacological approach. J Neurosci 26: 1331–1333.

Olsen TS (1995). Pathophysiology of the migraine aura: the spreading depression theory. Brain 118: 307–308.

Paoletti P, Neyton J (2007). NMDA receptor subunits: function and pharmacology. Curr Opin Pharmacol 7: 39–47.

Peeters M, Gunthorpe MJ, Strijbos PJ, Goldsmith P, Upton N, James MF (2007). Effects of pan- and subtype-selective N-methyl-D-aspartate receptor antagonists on cortical spreading depression in the rat: therapeutic potential for migraine. J Pharmacol Exp Ther 321: 564–572.

Peixoto NL, Fernandes de Lima VM, Hanke W (2001). Correlation of the electrical and intrinsic optical signals in the chick spreading depression phenomenon. Neurosci Lett 299: 89–92.

Peltz G, Pacific DM, Noviasky JA, Shatla A, Mehalic T (2005). Seizures associated with memantine use. Am J Health Syst Pharm 62: 420–421.

Petzold GC, Windmüller O, Haack S, Major S, Buchheim K, Megow D *et al.* (2005). Increased extracellular K+ concentration reduces the efficacy of N-methyl-D-aspartate receptor antagonists to block spreading depression-like depolarisations and spreading ischemia. Stroke 36: 1270–1277.

Risher WC, Ard D, Yuan J, Kirov SA (2010). Recurrent spontaneous spreading depolarisations facilitate acute dendritic injury in the ischemic penumbra. J Neurosci 30: 9859–9868.

Sakowitz OW, Kiening KL, Krajewski KL, Sarrafzadeh AS, Fabricius M, Strong AJ *et al.* (2009). Preliminary evidence that ketamine inhibits spreading depolarisations in acute human brain injury. Stroke 40: e519–e522.

Sheardown MJ (1993). The triggering of spreading depression in the chick retina: a pharmacological study. Brain Res 607: 189–194.

Sun L, Shipley MT, Lidow MS (2000). Expression of GLUN1, NR2A-D, and NR3 subunits of the NMDA receptor in the cerebral cortex and olfactory bulb of adult rat. Synapse 35: 212–221.

Thompson CL, Drewery DL, Atkins HD, Stephenson FA, Chazot PL (2002). Immunohistochemical localization of N-methyl-D-aspartate receptor subunits in the adult murine hippocampal formation: evidence for a unique role of the NR2D subunit. Brain Res Mol Brain Res 102: 55–61.

Van den Maagdenberg AM, Pietrobon D, Pizzorusso T, Kaja S, Broos LA, Cesetti T *et al*. (2004). A Cacna1a knockin migraine mouse model with increased susceptibility to cortical spreading depression. Neuron 41: 701–710.

Vitanova LA (2011). Immunocytochemical study of GLUN1, NR2A and NR2B subunits of NMDA receptor in frog retina (Rana ridibunda). Acta Histochem 13: 495–500.

Willette RN, Lysko PG, Sauermelch CF (1994). A comparison of (+)SK&F 10047 and MK-801 on cortical spreading depression. Brain Res 648: 347–351.

Yamakura T, Mori H, Masaki H, Shimoji K, Mishina M (1993). Different sensitivities of NMDA receptor channel subtypes to non-competitive antagonists. Neuroreport 4: 687–690.